Constructing the Universe with Clusters of Galaxies, IAP 2000 meeting, Paris (France) July 2000
Florence Durret & Daniel Gerbal eds.

THERMAL AND NON-THERMAL PHENOMENA IN GALAXY CLUSTERS

S. COLAFRANCESCO
Osservatorio Astronomico di Roma, Via Frascati, 33
Monteporzio (Roma) - ITALY

Galaxy clusters are astrophysical systems which host different physical phenomena of thermal and non-thermal origin. Here we discuss a few arguments which relate the presence of Cold dark Matter with the existence of non-thermal phenomena in these cosmic structures. Specifically, we discuss here the origin of extended cluster radio halos in a model in which neutralinos, χ, are assumed to be the best candidates for the Cold Dark Matter. We finally show that the next generation gamma-ray experiments have the power to discriminate among different models for the origin of non-thermal phenomena in galaxy clusters.

1 Thermal and Non-thermal Phenomena in Clusters

Most of the knowledge we have about galaxy clusters comes from the optical (typical energies of a few eV) and X-ray (mostly the range $0.1 - 10$ keV) bands where the emission mechanisms are mainly due to thermal phenomena. However, soon as we go beyond these energy ranges, we discover the existence of a variety of other phenomena mainly of non-thermal origin. In fact:
• more than 40 clusters (of different dynamical and physical state) show the presence of radio halos and/or relics powered by synchrotron emission of relativistic electrons (see, e.g., Feretti at this meeting);
• excesses of emission over the thermal one have been discovered in several nearby clusters in the EUV (Lieu et al. 1996) and hard X-rays (Fusco-Femiano et al 1999, 2000; Rephaeli, Gruber and Blanco 1999, Kaastra et al. 1999). These are possibly due to Inverse Compton Scattering (ICS) of relativistic electrons or - more likely - to bremsstrahlung emission of suprathermal electrons (Dogiel 1999, 2000; Sarazin and Kempner 1999; Blasi 1999), as discussed by C. Sarazin at this meeting;
• appreciable gamma-ray fluxes are expected from nearby clusters either due to electron bremsstrahlung or to π^0 decay (see, e.g., discussion in Colafrancesco and Blasi 1998) - or to a combination of these two mechanisms - but not yet definitely detected (Sreekumar et al. 1996).

The picture emerging is that of an ICM which is stratified in its energy content in a thermal, a suprathermal and a relativistic population of particles. Disentangling the energy structure of the ICM requires multiwavelength observations from radio to gamma rays, these last observations being crucial to assess the role of the different electron populations of low and high energies. In

fact, the presence of suprathermal and/or relativistic electrons and protons reflects in different fluxes and energy spectra in the emission of clusters at $E > 100$ MeV (see Fig.1). Bremsstrahlung

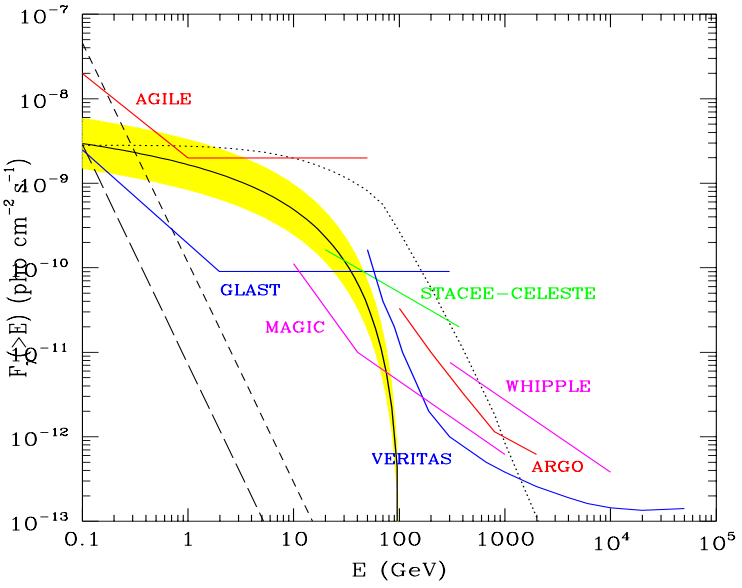

Figure 1: The gamma-ray emission predicted from $\chi\chi$ annihilation in Coma (solid curve) as calculated by Colafrancesco & Mele (2000) is compared to the sensitivities of the operating and planned gamma ray experiments. A neutralino with mass $M_\chi = 100$ GeV has been assumed. The shaded area shows the uncertainty in the gammma-ray spectrum due to an uncertainty of a factor 2 in the normalization of the π^0 source spectrum (see Colafrancesco & Mele 2000 for details). The short and long dashed curves refer to the gamma ray emission produced by relativistic bremmstrahlung of a population of primary cosmic rays and are calculated using the formula given in Sreekumar et al. (1996) for two choices of the Coma magnetic field:: $B = 0.3\mu$G and $B = 1\mu$G, respectively. The dotted curve is the gamma-ray emission produced by $\pi^0 \rightarrow \gamma + \gamma$ decay from pp collision in the ICM according to Colafrancesco & Blasi (1998) and Blasi & Colafrancesco (1999).

emission can be detectable up to ~ 1 GeV while gamma-rays from π^0 decay extends up to ~ 100 GeV (for the case of the annihilation of neutralinos with $M_\chi \sim 100$ GeV) or even up to $\sim 10^3$ GeV (for the case of $pp \rightarrow \pi^0$ collision in the ICM). The next generation gamma-ray instruments will have the capabilities to test in detail the energy stratification of the ICM and the relevance of non-thermal phenomena in galaxy clusters. These observations will also have a large impact in assessing the possible cosmological relevance of non-thermal phenomena, a line of investigation which has been recently initiated (see, e.g., Colafrancesco 1999, 2000a, Loeb & Waxman 2000). In this line, it has been suggested that the presence of a non-thermal population of electrons has a non-negligible impact on the thermal content of clusters (Colafrancesco 2000b) influencing also the shape of the $L_X - T$ relationship especially at low T, and on the evaluation of the cluster masses (total and gas) and baryonic fractions, since each electron population contributes to the total ICM pressure separately (Colafrancesco 1998-2000a, Kaastra et al. 1999). However, the connection between non-thermal physics and the cluster structure and dynamics is still committed to have a detailed description of the cosmic ray population in the ICM and of the interaction properties of the DM particles.

Here we want to discuss, briefly, a few arguments which relate the presence and the physical properties of the Cold Dark Matter with the existence of non-thermal phenomena in galaxy clusters. Specifically, we discuss here the origin of extended cluster radio halos in a model in which neutralinos, (χ the lightest supersymmetric particles), are assumed to be the best candidates for the Cold Dark Matter.

2 Neutralinos and the origin of radio halos in galaxy clusters

Clusters of galaxies are the largest bound systems which have indeed both the largest amount of DM and extended Intra Cluster (IC) magnetic field at the level of at least a few μG, as probed by Faraday rotation measurements (Eilek 1999; Vallee et al. 1986, 1987; see Kronberg 1995 for a review). The decays of $\chi\chi$ annihilation products (fermions, bosons, etc.) yield, among other particles, energetic electrons and positrons (hereafter referred as electrons) up to energies comparable to the neutralino mass (usually of the order of tens to hundreds GeV). These electrons can emit synchrotron radiation in a DM halo which is filled with a magnetic field at the level of μG. It is then natural to expect that the χ annihilation products can give origin to a diffuse, extended radio emission.

The detailed interaction properties of the neutralino are determined once its physical composition is fixed (indeed, neutralinos are a linear combinations of two Higgsinos and two gauginos). Recent analysis of accelerator constraints, combined with cosmological DM requirements (Ellis et al. 2000), points to: *i*) a lightest neutralino heavier than about 46 GeV; *ii*) a lightest neutralino that is either a *pure* gaugino or a heavily mixed gaugino-Higgsino state, since a predominantly Higgsino state cannot provide a substantial component of the Dark Matter. Neutralinos decouple from the primeval plasma when they are no longer relativistic. Their present abundance can be calculated by solving the Boltzmann equation for the evolution of the density of particle species (see, e.g., Kolb and Turner 1990). Both the neutralino mass and its physical composition affect in general the rate and the final state composition of the $\chi\chi$ annihilation process. The annihilation rate of neutralinos in a DM halo is $R = n_\chi(r)\langle\sigma V\rangle_A$, where $n_\chi(r)$ is the neutralino number density and $\langle\sigma V\rangle_A$ is the $\chi\chi$ annihilation cross section averaged over a thermal velocity distribution at freeze-out temperature. Although the $\chi\chi$ annihilation cross section is a nontrivial function of the mass and physical composition of the neutralino, to our purpose it suffices to recall that the χ relic density is approximately given by $\Omega_\chi h^2 \simeq \frac{3\times10^{-27}\ \mathrm{cm^3\ s^{-1}}}{\langle\sigma V\rangle_A}$ (Jungman et al. 1996). Hence, for the $\chi\chi$ annihilation, we will assume a total χ cross section of $\langle\sigma V\rangle_A \approx 10^{-26}\ \mathrm{cm^3\ s^{-1}}$ to be consistent with the value $\Omega_m \sim 0.3$ derived from clusters of galaxies and large scale structure constrains (see, e.g., discussion in Bahcall 1999; Turner 1999).

Neutralinos which annihilate in a DM halo produce quarks, leptons, vector bosons and Higgs bosons, depending on their mass and physical composition. Monochromatic electrons (with energy about M_χ), coming from the direct channel $\chi\chi \to ee$, are in general much suppressed (Turner and Wilczek 1990). Electrons are then produced from the decay of the final heavy fermions and bosons. The different composition of the $\chi\chi$ annihilation final state will in general affect the form of the final electron spectrum. Following Colafrancesco and Mele (2000), we calculated the production spectrum, $Q_e(E,r)$, of electrons in two somewhat extreme cases: 1) a pure-gaugino annihilation, which yields mainly fermion pair direct production $\chi\chi \to ff$; 2) a mixed gaugino-higgsino state in the case of a dominant annihilation into W (and Z) vector bosons, $\chi\chi \to WW(ZZ)$. A real situation will be mostly reproduced by either of the above two cases, or by a linear combination of the two.

2.1 The production of electrons from $\chi\chi$ annihilation

The total source spectra in the two cases considered are shown in Fig.2 for $M_\chi = 100$GeV. The heavy solid curve is the total spectrum for the model in which fermions dominate the annihilation. We also show the different contributions to the total source spectra from fermions, i.e. the source spectrum for first-generation prompt electrons (P1), second-generation prompt electrons (P2) and secondary electrons produced in the decay of charged pions (π). The total source spectrum is rather smooth and, when approximated by a single power-law, it has an overall slope $Q_e \sim E^{-1.9}$ in the interesting energy range $0.02 \leq E/M_\chi \leq 0.7$.

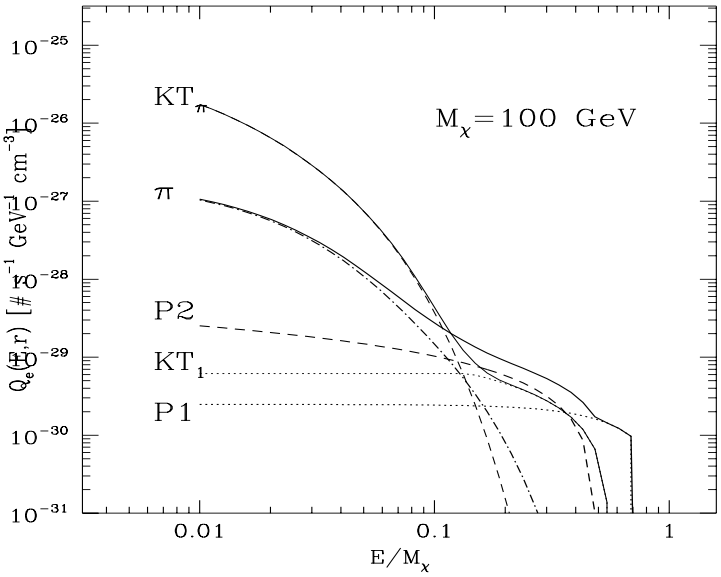

Figure 2: The source spectrum for a model in which fermions dominate the neutralino annihilation products ($\chi\chi \to ff$): first generation, prompt electrons (P1), second generation, prompt electrons (P2) and secondary electrons produced in the decay of charged pions (π). The light solid curve is the total source spectrum for this case. We also show the source spectra for the model in which gauge bosons dominate the annihilation. The contributions from the decays ($W^\pm \to \tau^\pm \to e^\pm$, $W^\pm \to c \to e^\pm$) and from the decays of charges pions produced in hadronic decays of $W^\pm$ and Z^0 bosons are labeled $\mathrm{KT_1}$ (light dotted curve) and KT_π (light dashed curve), respectively. The light solid curve is the total source spectrum for the case ($\chi\chi \to WW$). A neutralino density $n_\chi = 1$ cm^{-3} and annihilation cross section $\langle\sigma V\rangle_A = 10^{-27}$ cm^3 s^{-1} have been used in this plot.

The source spectra for the model in which gauge bosons dominate the annihilation is given by the light solid curve. For this case we show the contributions from the decay $W^\pm \to \tau^\pm \to e^\pm$; $W^\pm \to c \to e^\pm$ (labeled as $\mathrm{KT_1}$) and from the decays of charged pions produced in hadronic decays of the $W^\pm$ (labeled with KT_π). Note that we make this analysis restricting only to the WW channel, since the ZZ contribution gives rise to a qualitatively similar spectrum.

Two prominent spectral features (bumps) around $E \sim M_\chi/2$ (arising from the direct decay $W \to e\nu$) and $E \sim M_\chi/20$ are shown by the model in which gauge bosons dominate the annihilation, in comparison with the smoother spectral shape of the fermion dominated annihilation. From a closer inspection of Fig. 2, one can see that the main difference between the two models stands in the height and width of the bumps at energies below $M_\chi/10$, where the pion-produced electrons dominate the source spectrum, and in the high-energy tail at $E \lesssim 0.7 M_\chi$ where the P1 contribution dominates. In both models, electrons produced by tertiary decays of gauge bosons are neglected because their contribution is subdominant with respect to the pion decay distribution.

In the calculation of the radio halo emission (see below) the source spectra of will be multiplied by a factor 2 to take into account the contribution of both electrons and positrons.

2.2 The radio halo emission

The time evolution of the electron spectrum is given by the transport equation:

$$\frac{\partial n_e(E,r)}{\partial t} - \frac{\partial}{\partial E}\Big[n_e(E,r)b(E)\Big] = Q_e(E,r) \qquad (1)$$

where $n_e(E,r)$ is the equilibrium spectrum at distance r from the cluster center for the electrons with energy E. The source spectrum, $Q_e(E,r)$, rapidly reaches its equilibrium configuration

mainly due to synchrotron and Inverse Compton Scattering (hereafter ICS) losses at energies $E \gtrsim 150$ MeV and to Coulomb losses at smaller energies (see, e.g., Blasi and Colafrancesco 1999). Since these energy losses are efficient in the ICM and DM annihilation continuously refills the electron spectrum, the population of high-energy electrons can be described by a stationary transport equation

$$-\frac{\partial}{\partial E}\Big[n_e(E,r)b(E)\Big] = Q_e(E,r) \ , \tag{2}$$

from which the equilibrium spectrum can be calculated. Here, the function $b(E)$ gives the energy loss per unit time at energy 2¡ E

$$b_e(E) = \left(\frac{dE}{dt}\right)_{ICS} + \left(\frac{dE}{dt}\right)_{syn} + \left(\frac{dE}{dt}\right)_{Coul} = b_0(B_\mu)E^2 + b_{Coul} \ , \tag{3}$$

where $b_0(B_\mu) = (2.5 \cdot 10^{-17} + 2.54 \cdot 10^{-18} B_\mu^2)$ and $b_{Coul} = 7 \times 10^{-19}[n(r)/10^{-3} cm^{-3}]$ (here b_e is given in units of GeV/s and the IC gas density, $n(r)$, in units of 10^{-3} cm^{-3}).

Electrons with energy E radiate typically at a frequency

$$\nu \approx 3.7 \text{ MHz } B_\mu \left(\frac{E}{\text{GeV}}\right)^2 \ . \tag{4}$$

The radio emissivity at frequency ν and at distance r from the cluster is evaluated from eqs.(2-4) and reads:

$$j(\nu, r) = n_e(E,r) \left(\frac{dE}{dt}\right)_{syn} \ . \tag{5}$$

Its volume integral yields the radio halo luminosity, $J(\nu) = \int dV j(\nu, r)$, which is the quantity directly comparable to the available observations (here dV id the volume element of the cluster).

3 A panorama of definite predictions

It is noticeable that a model derived entirely from the fundamental properties of DM particles and from general cluster properties - like the model presented here for the origin of radio halos in clusters - can reproduce successfully (see Fig.3) the spectra of the radio halo emission observed from Coma (Giovannini et al. 1993, Deiss et al. 1997) and 1E0657-56 (Liang et al. 2000). The slope and the frequency extension of the radio halo spectra can set interesting constrains on the neutralino mass and composition. In fact, the highest observed frequency of the radio halo spectrum sets a lower limit to the neutralino mass: $M_\chi \geq 16.44 \text{ GeV } k^{-1}\left[\left(\frac{\nu_{max,obs}}{GHz}\right)\frac{1}{B_\mu}\right]^{1/2}$, with $k \approx 0.7$. In particular, the highest frequency at which the Coma spectrum has been observed requires $M_\chi \geq 54.6$ GeV $B_\mu^{-1/2}$. A more stringent limit, $M_\chi \geq 70.5$ GeV $B_\mu^{-1/2}$, is obtained from the cluster 1E0657-56. Radio halo observations at frequencies larger than $5 \div 10$ GHz are not yet available, but are important to test the present model. In fact, the detection of a true high frequency cutoff, ν_{cut}, in the radio halo spectra would give an upper limit on the neutralino mass.

In the same framework, the slope of the radio halo spectrum gives an indication on the neutralino physical composition. The radio halo spectra of the two clusters considered here are well fitted by a model in which the neutralinos behave like pure gauginos, and annihilate mainly into fermions. On the other hand, when the $\chi\chi$ annihilation is dominated by vector bosons (implying a non-negligible higgsino component), the electron source spectrum is too steep and shows two unobserved bumps at low and high energies (see Fig.3). Indeed, Fig.3 shows also how far the χ model dominated by vector bosons is from reproducing the data of the radio halo spectrum of Coma and 1E0657-56.

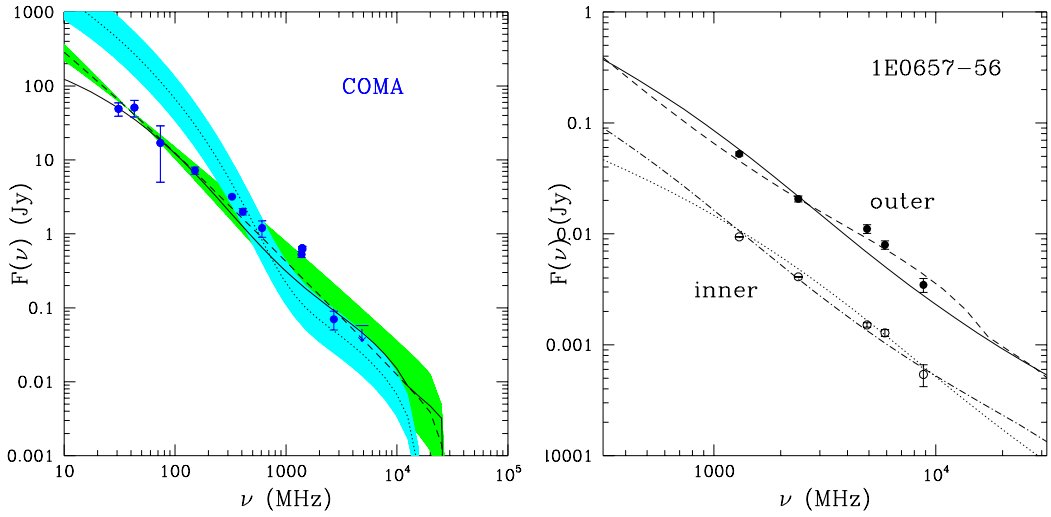

Figure 3: **Left** The Coma radio halo spectrum predicted in a model in which χ annihilation is dominated by fermions ($\chi\chi \to ff$; solid curve) is compared to the model in which annihilation is dominated by higgsinos ($\chi\chi \to WW$; dotted curve). The power-law approximation for the case $\chi\chi \to ff$ is also shown (dashed curve). The curves are plotted for a radially decreasing magnetic field with central value $B_0 = 8\mu$G. A constant core profile with $r_c = 0.4 h_{50}^{-1}$ Mpc, $\beta = 0.76$ has been adopted. The radio halo emission has been integrated out to $1.3 h_{50}^{-1}$ Mpc. Data are taken from Deiss et al. (1997). Shaded areas enclose radio halo spectra evaluated considering both an uncertainty of a factor ± 2 in normalization and $\pm 10\%$ in the slope of the source spectra. **Right** The radio halo spectrum of the cluster 1E0657-56 in the inner (empty circles) and outer (filled circles) regions. Dashed and dot-dashed curves are for a uniform field $B_{uniform} = 2\mu$G and $B_{uniform} = 9\mu$G, respectively. Solid and dotted curves are for a magnetic field with a radial dependence $B = B_0 \left[1 + (r/r_{c,B})^2\right]^{-0.5}$ with a central amplitude $B_0 = 100\mu$G and $B_0 = 90\mu$G, respectively. Curves are shown for a model in which neutralino annihilation is dominated by fermions ($\chi\chi \to ff$). Constant core density profiles have been adopted here with parameters $R_{halo} = 2 h_{50}^{-1}$ Mpc, $r_c = 0.38 h_{50}^{-1}$ Mpc, $\beta = 0.7$ and $n_{\chi,0} = 9 \cdot 10^{-3}$ cm^{-3} for the outer region and $R_{halo} = 0.6 h_{50}^{-1}$ Mpc, $r_c = 0.08 h_{50}^{-1}$ Mpc, $\beta = 0.49$ and $n_{\chi,0} = 9 \cdot 10^{-3}$ cm^{-3} for the inner region (see Liang et al. 2000). Data are from Liang et al. (2000).

Other interesting properties of the model we present in this paper are its ability to reproduce the spatial extension of the radio halo brightness and its correlation with the X-ray brightness of the cluster, and the observed correlation between the monochromatic radio halo power, $J_{1.4}$, and the IC gas temperature, T (see Colafrancesco & Mele 2000 for details). The steep $J_{1.4} - T$ relation shown by the available radio-halo clusters can be reproduced as a superposition of evolutionary effects of the correlation $J_{1.4} \sim T^q$, with $q \sim 4.2 \div 4.4$, which results from the dependence of the electron spectrum, $n_e(E, r) \propto n_\chi^2(r) \langle \sigma V \rangle_A$, from the DM density, $n_\chi(r)$, and annihilation cross-section, $\langle \sigma V \rangle_A$, with the further assumption of an energy equipartition between the IC gas and the IC magnetic field (see Fig.4 and Colafrancesco & Mele 2000 for further details).

Another remarkable feature of the present model, is that neutralino annihilation can also give rise to gamma rays with continuum fluxes which are overwhelmingly due to $\pi^0 \to \gamma + \gamma$ decays (see Fig.5). The gamma ray emission produced by $\chi\chi$ interaction extends up to energies corresponding to the neutralino mass. Thus, a way to disentangle a particular model for the cluster gamma-ray emission is provided by the future high-energy gamma-ray experiments. They will allow to observe galaxy clusters with a photon statistics sufficient to disentangle the gamma-ray spectra produced by the $\pi^0 \to \gamma + \gamma$ electromagnetic decay, as predicted either in DM annihilation models ($\chi\chi \to ff, WW \to \pi^0$) or in secondary electron models ($pp \to \pi^0$; see, e.g., Colafrancesco and Blasi 1998), from the gamma-ray emission produced by the bremsstrahlung

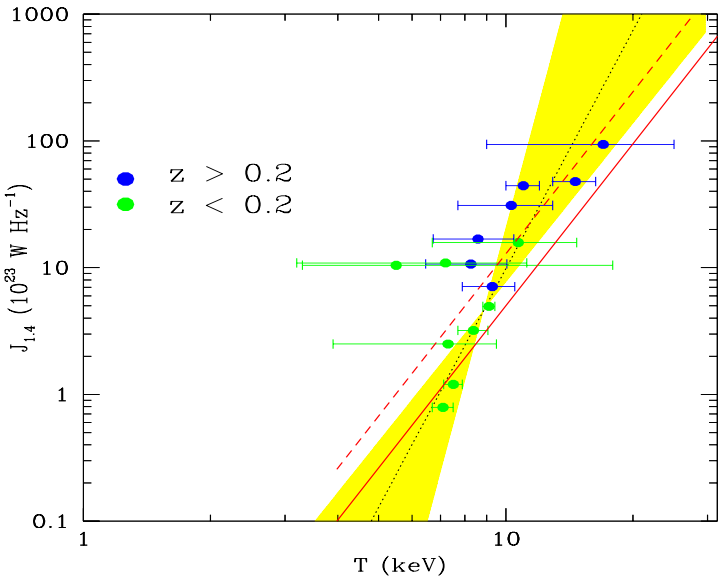

Figure 4: The $J_{1.4} - T$ correlation is shown for the radio halo clusters at $z > 0.2$ (dark dots) and at $z < 0.2$ (gray dots). The dotted line is the best fit power-law to the data (the shaded area contain the uncertainty region of the best fit points). The heavy lines are the relations $J_{1.4} \sim T^{4.25}$ expected in the neutralino annihilation model discussed in the paper and are evaluated at $z = 0$ (solid) and at $z = 0.25$ (dashed), respectively. data are taken from Feretti (1999), Giovannini et al. (1999), Liang (1999), Owen et al. (1999).

of primary cosmic ray electrons (see Fig.1).

Finally, we want to mention a number of additional stringent predictions through which the model discussed here can be tested.

(i) According to the fact that DM is present in all large scale structures, we should observe radio halos in every cluster, which is not actually observed. However, the radio halos can be fitted with sensitively high magnetic fields (with central values $B_0 \sim 5 \div 100$ μG). So, only clusters which have such high magnetic fields can show a bright radio halo. All the other clusters are expected to have faint radio halos that can brighten up when there is some effect that raises the magnetic field amplitude, for example, a merging event (see the numerical simulations of K. Roettiger, 1999).

(ii) A possible problem could be given by the fact that cooling flow clusters, which have usually high magnetic field in their central cooling regions, do not show strong evidence for extended radio halos. However, if one assumes that the magnetic field in cooling-flow clusters is quite peaked near the cluster center and decreases rapidly towards the outskirts, the radio halo emission predicted in the present model is a factor $\sim 10^2 \div 10^6$ lower than that of a non-cooling flow cluster with the same mass [these estimates are obtained for a Coma-like cluster using $B(r) \sim r^{-1}$ with a scale length of $r_{c,B} = 0.1 h_{50}^{-1}$ Mpc , see Colafrancesco & Mele 2000, for details]. Nonetheless, it remains true that our model does predict that cooling flow cluster should possess small-size, low-luminosity and low-surface brightness radio halos.

(iii) Under the assumption that all clusters show a universal DM profile, the radio halo spectrum is basically the same unless the magnetic field configuration of the cluster is very peculiar. For example, steep radio halo spectra can be obtained mainly due to the presence of magnetic fields that decrease strongly from the cluster center.

Little is known about the presence and structure of the IC magnetic fields. Faraday rotation measurements (Vallee et al. 1986, 1987; Eilek 1999) give a lower limit to the magnetic field in small scale regions of the cluster (Dolag et al. 1999), and we could have to deal with large scale IC magnetic fields that are lower than those ($B_0 \sim 5 \div 100$ μG, $B_{uniform} \sim 1 \div 3$ μG) required by

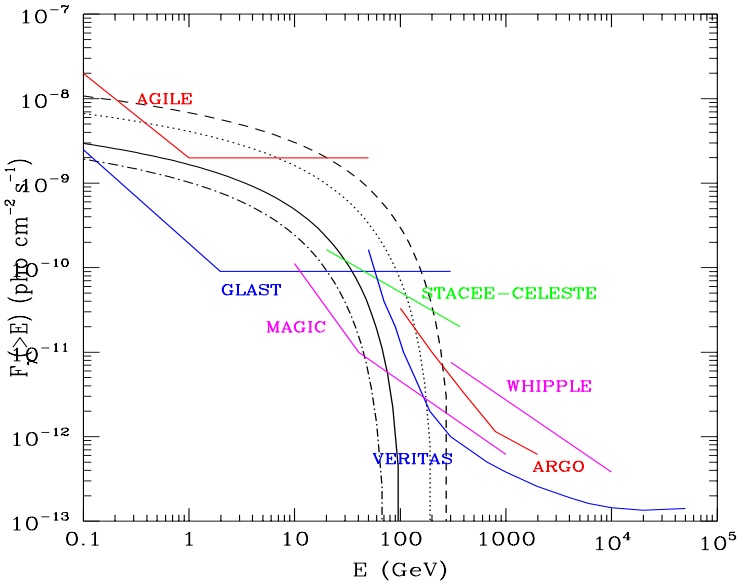

Figure 5: The gamma-ray emission predicted from $\chi\chi$ annihilation in galaxy clusters (solid curve) calculated for different neutralino masses: $M_\chi = 70$ GeV (dot-dashed curve), $M_\chi = 100$ GeV (solid curve), $M_\chi = 200$ GeV (dotted curve) and $M_\chi = 300$ GeV (dashed curve). The sensitivities of the operating and planned gamma ray experiments are also shown. Combined gamma ray observations of clusters from ~ 1 GeV to 500 GeV can clearly determine the neutralino mass from both the intensity of the spectrum and its high-energy cutoff (see Colafrancesco & Mele 2000 for details).

the present model to explain radio halos. However, even in the case in which the magnetic field are not so strong in clusters, the present model certainly yields a natural explanation for the origin of the *seed* high-energy electrons, which are a necessary input for any model of radio halo (and relic) formation. The diffuse radio emission due to such a population of seed electrons could then be boosted by the amplification of the IC magnetic field subsequent to a strong cluster merger (see, e.g., Roettiger 1999), or the seed electrons could be reaccelerated by intracluster turbulence (Deiss et al. 1997, Eilek and Weatherall 1999, Brunetti et al. 1999).

While at the moment, we observe radio halos in more than 40 clusters at different redshifts, the definite test for the theory of the radio halo origin proposed here is committed to obtain a larger, unbiased survey of galaxy clusters through high radio sensitivity observations. This search should be complemented with the search for gamma-ray emission from galaxy clusters whose predicted intensity is matched by the sensitivities of the next generation gamma-ray experiments (GLAST, AGILE, MAGIC, VERITAS, ARGO, STACEE).

In conclusion, we want to emphasize that the astrophysical expectations from the $\chi\chi$ annihilation are consistent, at the moment, with the constrains set by all the available observations on clusters containing radio halos. The astrophysical and fundamental physics requirements on the model discussed here are stringent, but still well allowed. It is appealing, in these respects, to expect that some astrophysical features of galaxy clusters might give information on the fundamental properties of the DM particles.

References

1. Bahcall, N. 1999, preprint astro-ph/9901076
2. Blasi, P., 1999, ApJ, 525, 603
3. Blasi, P. and Colafrancesco, S. 1999, Astroparticle Physics, 12, 169
4. Brunetti, G.,Feretti, L., Giovannini, G. and Setti, G. 1999, in 'Diffuse Thermal and Rela-

tivistic Plasma in Galaxy Clusters', MPE Report 271, p.263
5. Colafrancesco, S. and Blasi, P. 1998, Astroparticle Physics, 9,227
6. Colafrancesco, S. 1999, in 'Diffuse Thermal and Relativistic Plasma in Galaxy Clusters', MPE Report 271, p.295
7. Colafrancesco, S. 2000a, in "Large Scale Structure in the X-Ray Universe", M. Plionis and I. Georgantopoulos Eds., p.179
8. Colafrancesco, S. 2000b, in "Frontier Objects Between Astrophysics and Particle Physics', in press
9. Colafrancesco, S. & Mele, B. 2000, ApJ, submitted (astro-ph/0008127)
10. Deiss, B. et al. 1997, A&A, 321, 55
11. Dogiel, V. in 'Diffuse Thermal and Relativistic Plasma in Galaxy Clusters', MPE Report 271, p.259
12. Dolag, K.,Bartelmann, M. and Lesch, H. 1999, A&A, 348, 351
13. Eilek, J. 1999, in 'Diffuse Thermal and Relativistic Plasma in Galaxy Clusters', MPE Report 271, p.71
14. Eilek, J. and Weatherall, J.C. 1999, in 'Diffuse Thermal and Relativistic Plasma in Galaxy Clusters', MPE Report 271, p.249
15. Ellis, J., Falk, T., Ganis, G., and Olive, K.A. 2000, preprint hep-ph/0004169
16. Fusco-Femiano, R. et al. 1999, ApJ, 513, L24
17. Fusco-Femiano, R. et al. 2000, ApJ, in press (astro-ph/0003141)
18. Giovannini, G. et al. 1993, ApJ, 406, 359
19. Jungman, G., Kamionkowski, M., and Griest, K. 1996, Phys. Rep. 267, 195
20. Kaastra, J.S., Lieu,R., Mittaz, J., Bleeker, J., Mewe, R., Colafrancesco, S. and Lockman, F. 1999, ApJ, 519, L119
21. Kolb, E.W. and Turner, M.S. 1990, 'The Early Universe', (Addison-Wesley)
22. Liang, H., Hunstead, R.W., Birkinshaw, M. and Andreani, P. 2000, preprint astro-ph/0006072
23. Lieu, R. et al. 1996, Science, 274, 1335
24. Loeb, A. & Waxman, E. 2000, preprint astro-ph/0003447
25. Rephaeli, Y., Gruber, D. and Blanco, P. 1999, ApJ, 511, L21
26. Roettiger, K. 1999, in 'Diffuse Thermal and Relativistic Plasma in Galaxy Clusters', MPE Report 271, p. 231
27. Sarazin, C.L. and Kempner, J.C. 1999, ApJ, 533,73
28. Sreekumar, P. et al. 1996, ApJ, 464, 628
29. Vallee, J.P. et al. 1986, A&A, 156, 386
30. Vallee, J.P. et al. 1987, ApL, 25, 181